

MHD Simulations of Spheromaks and Low Aspect Ratio Tokamaks with Electrostatic Current Drive

Carl R. Sovinec, John M. Finn, and Diego del Castillo Negrete,

Los Alamos National Laboratory

A. Tarditi, D. D. Schnack

Science Applications International Corporation-San Diego

presented at the

41st Annual Meeting of the American Physical Society,
Division of Plasma Physics

November 15-19, 1999

ACKNOWLEDGMENTS

NIMROD code development team and advisors:

Ahmet Aydemir	IFS
James Callen	U-WI
Ming Chu	GA
John Finn	LANL
Tom Gianakon	LANL
Charlson Kim	CU-Boulder
Scott Kruger	SAIC
Jean-Noel Leboeuf	UCLA
Richard Nebel	LANL
Scott Parker	CU-Boulder
Steve Plimpton	SNL
Nina Popova	MSU
Dalton Schnack	SAIC
Carl Sovinec	LANL
Alfonso Tarditi	SAIC

Computations have been performed at

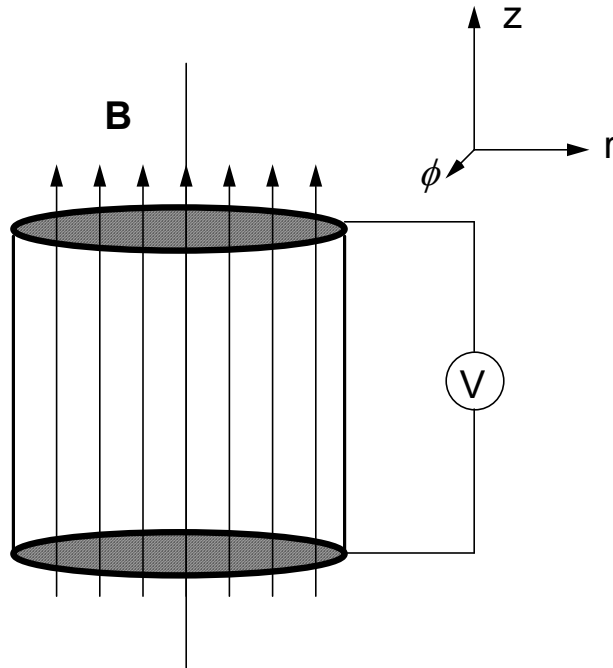
National Energy Research Scientific Computing Center, LBNL
Advanced Computing Laboratory, LANL

OBJECTIVES

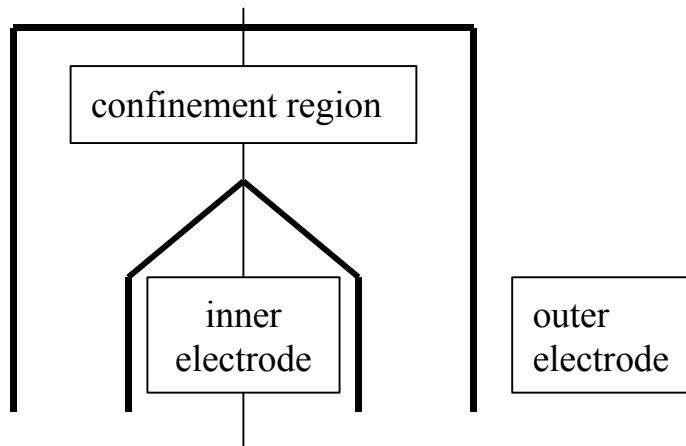
1. Describe the numerical solutions of fluid models for spheromak configurations, showing the nonlinear evolution from an unstable pinch to a sustained spheromak.
2. Examine the influence of including Hall and electron inertia terms in sustained configurations.
3. Determine what conditions lead to closed flux surfaces.
4. Examine the influence of geometry and plasma parameters on the flux conversion process.
5. Investigate the transition from spheromak to electrostatically driven, low aspect ratio tokamak through the addition of a central post and external current.

GEOMETRY

The geometry for simulating a "flux core" or "electrode" spheromak is a simple can with magnetic flux frozen into the top and bottom ends, which represent electrodes. Simulations with a central post are also based on this configuration.



Spheromaks driven with a plasma gun have concentric electrodes in the gun region and an open confinement region downstream.



FLUID MODELS

In most of the simulations presented here, the physical behavior of the system is modeled with the resistive MHD equations, where uniform density and vanishing pressure are assumed:

$$\rho \left(\frac{\partial \mathbf{V}}{\partial t} + \mathbf{V} \cdot \nabla \mathbf{V} \right) = \mathbf{J} \times \mathbf{B} + \nabla \cdot \rho \nu \nabla \mathbf{V}$$

$$\frac{\partial \mathbf{B}}{\partial t} = -\nabla \times \mathbf{E}$$

$$\mathbf{E} = \eta \mathbf{J} - \mathbf{V} \times \mathbf{B}$$

We have begun to investigate the importance of electron fluid effects with the Hall and electron inertia terms. Here the generalized Ohm's law is:

$$\mathbf{E} = \eta \mathbf{J} - \mathbf{V} \times \mathbf{B} + \frac{1}{en} \frac{(1 - m_e/m_i)}{(1 + m_e/m_i)} \mathbf{J} \times \mathbf{B} + \frac{1}{\varepsilon_0 \omega_p^2} \left[\frac{\partial \mathbf{J}}{\partial t} + \nabla \cdot (\mathbf{J} \mathbf{V} + \mathbf{V} \mathbf{J}) \right]$$

Gyroviscous terms have not been included in these simulations.

The equations are solved with the NIMROD simulation code.

- Two-fluid or single-fluid MHD equations
- Finite elements in the poloidal plane
- Pseudospectral, Fourier series representation of the toroidal direction
- Semi-implicit time advance
- Message-passing communication among processors
- Now publicly available from
 - <http://nimrodteam.org> or
 - <http://nimrod.saic.com>

SPHEROMAK BASICS

- Sustained spheromaks are driven by electrodes that are linked with magnetic flux.
- The electrostatic circuit applies a poloidal electric field and feeds-in toroidal flux, which compensates resistive dissipation in a sustained configuration.
- While both poloidal and toroidal current are driven directly by the applied poloidal electric field, Cowling's theorem applied to spheromaks states that purely axisymmetric poloidal flux in excess of the linked flux cannot persist under a steady applied potential.

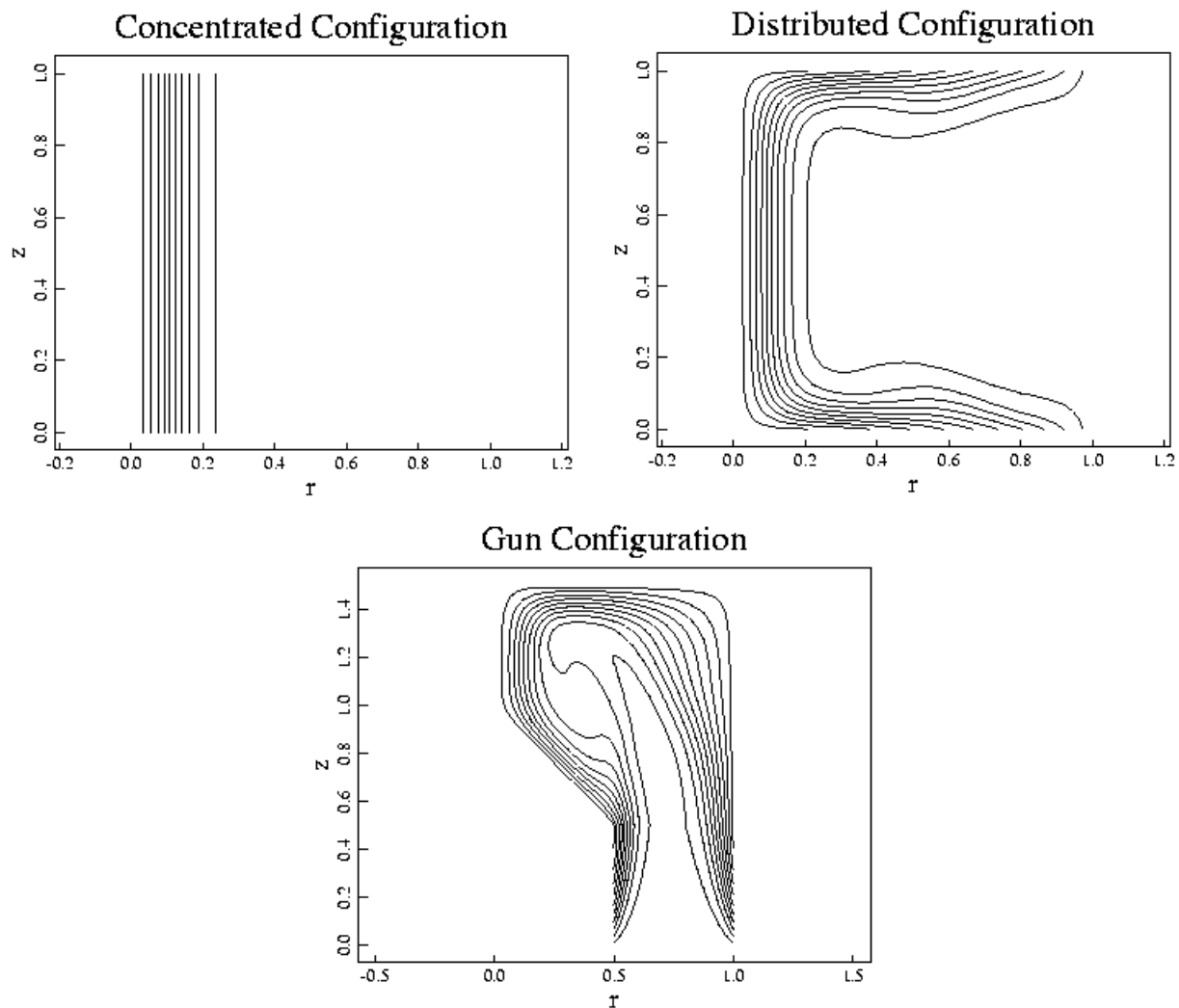
[See the discussion of poloidally symmetric reversal in Sect. II. A., "Single and multiple helicity Ohmic states in reversed-field pinches," Finn, Nebel, and Bathke, Phys. Fluids B **4**, 1262 (1992), and interpret the poloidal RFP direction as the toroidal spheromak direction, and vice versa.]

- The conversion of toroidal flux to poloidal flux observed in spheromak experiments must therefore result from nonsymmetric MHD (and/or Hall) effects or kinetic effects. [This work addresses fluid effects only.]
- If the configuration is symmetric, symmetry breaking result from instability. Here we demonstrate current-gradient driven activity that leads to spheromaks.

RELATING PINCHES AND SPHEROMAKS

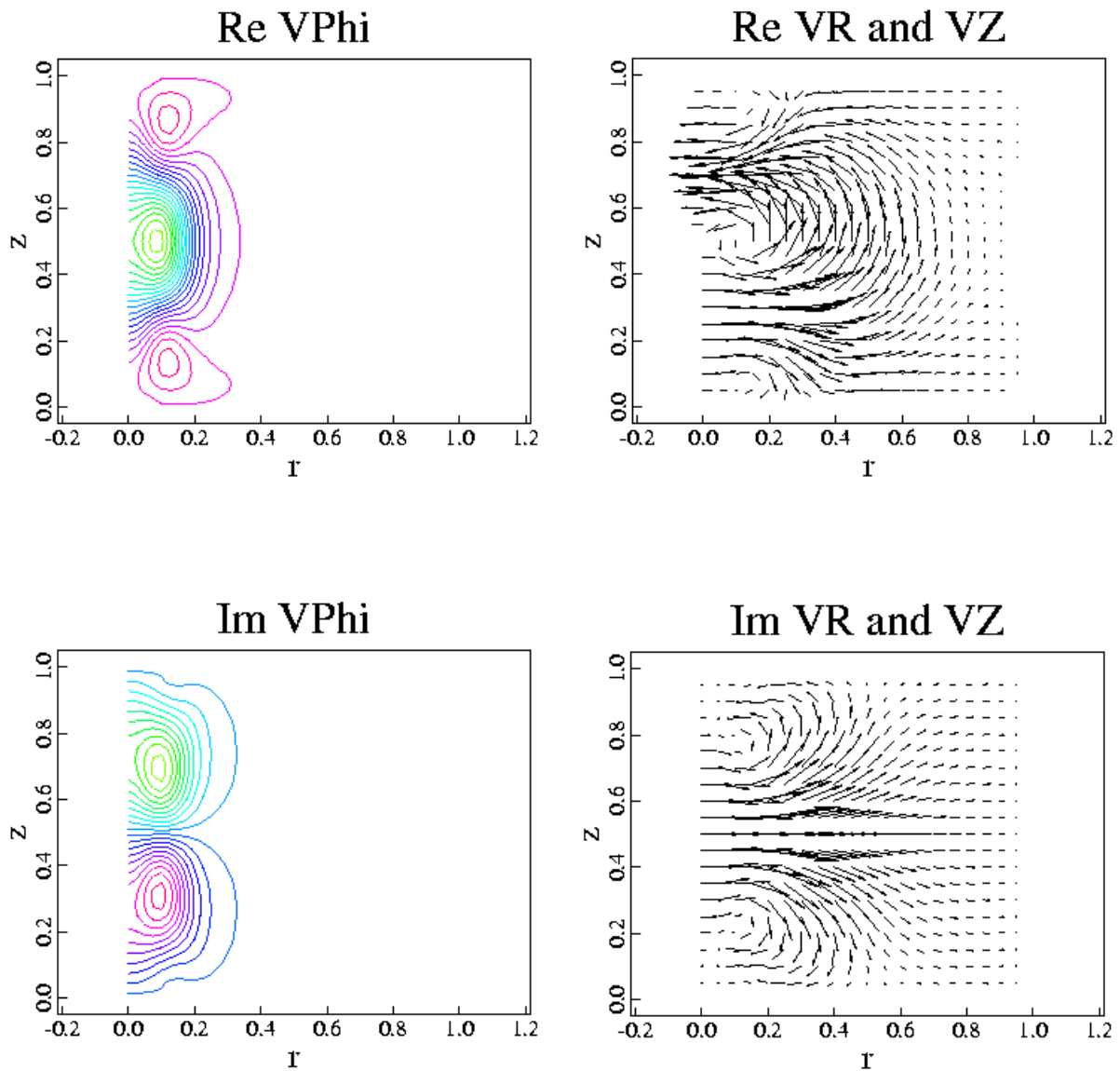
When the compressible 2D MHD equations are solved for conditions that lead to a spheromak, the result is a "stabilized" or paramagnetic pinch. The net electric field is poloidal, and force balance leads to concentrated poloidal flux.

Contour plots of poloidal flux illustrate this concentration in 2D simulations.



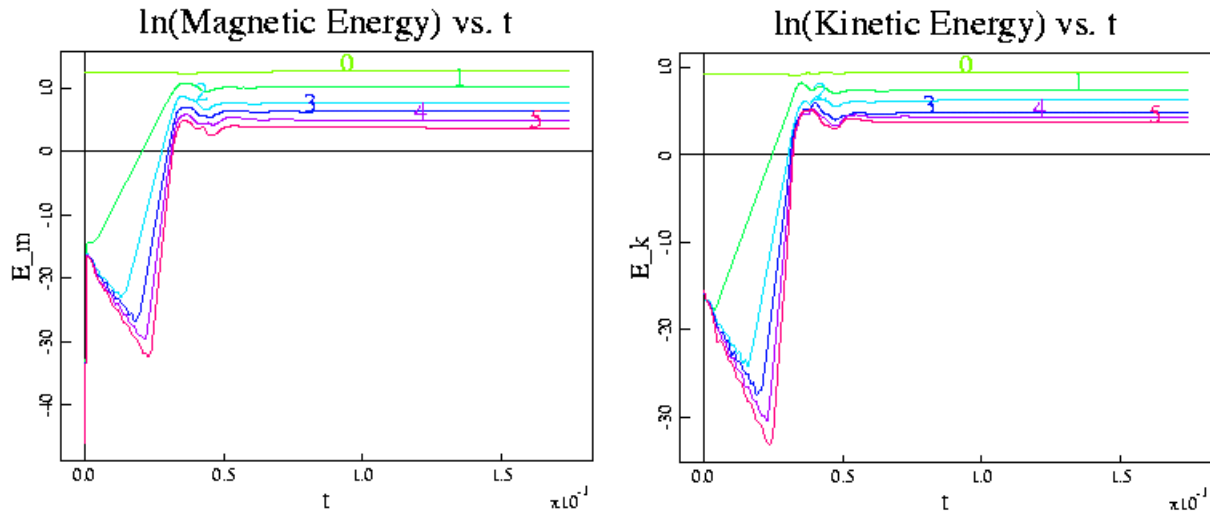
All of these configurations are unstable in resistive 3D MHD.

The growth rate and eigenfunction of the linear ($n=1$) mode of the pinch are strongly influenced by the field line tying conditions at the electrodes.

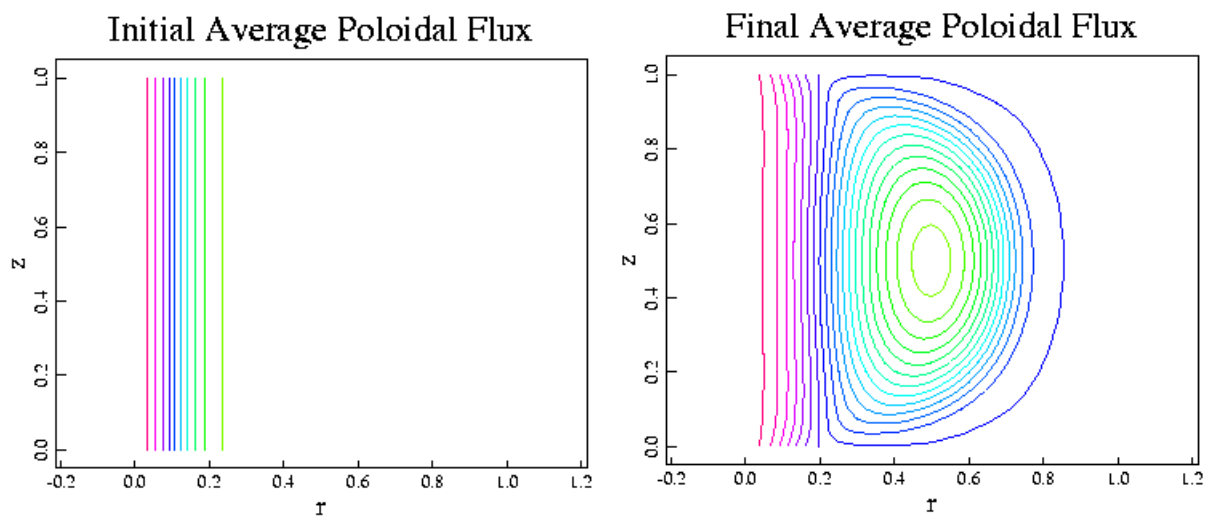


The linearly unstable eigenfunction of the "concentrated configuration."

Saturation of the instability results from feedback to the average field and from coupling to larger n .



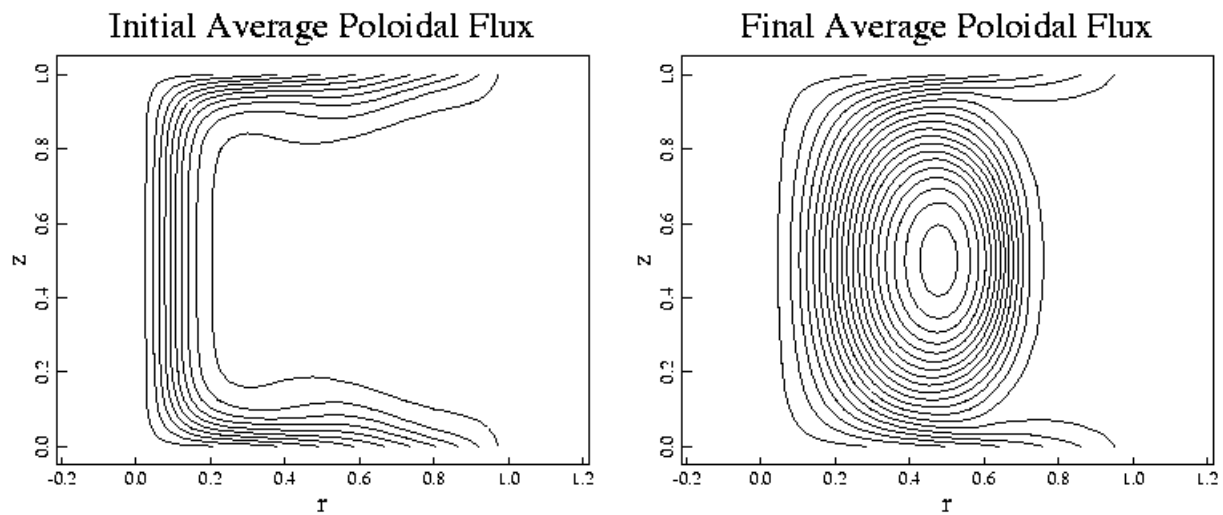
Evolution of fluctuation energy in the "concentrated configuration". Labels indicate n -number, and time is in diffusion times. The $n=1$ fluctuation dominates the saturated spectrum.



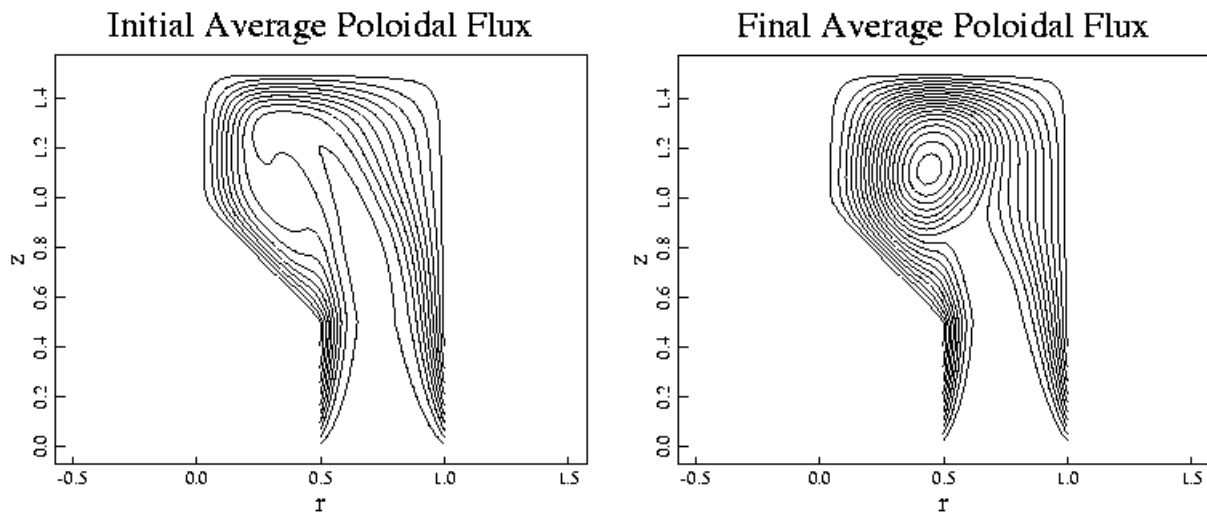
Saturation generates the spheromak configuration itself! MHD fluctuations convert toroidal flux to poloidal flux.

The "distributed" and "gun" configurations show qualitatively similar behavior when nonlinear 3D simulations with random perturbations are evolved from the 2D pinch states.

DISTRIBUTED CONFIGURATION

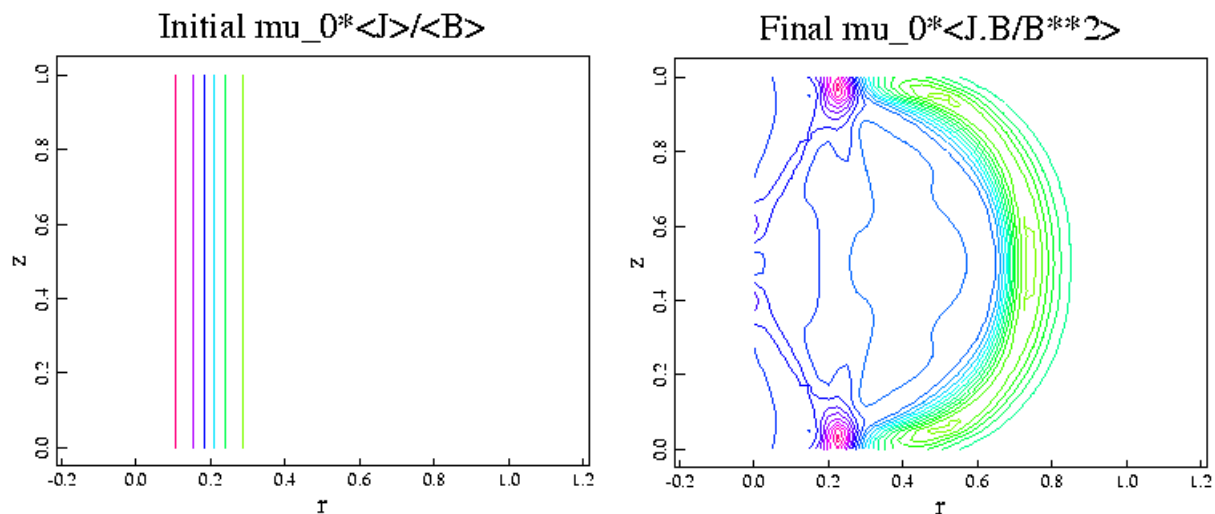


GUN CONFIGURATION

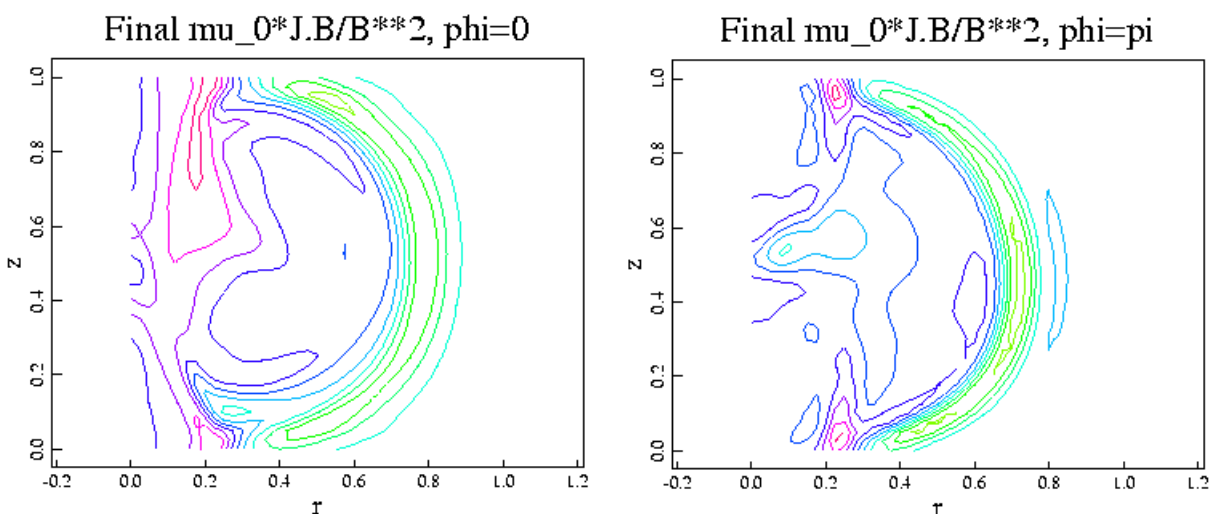


Saturation relaxes the parallel current profile from the initial pinch configuration, but the relaxation is incomplete, and $O(1)$ variations persist in this driven/damped system.

The "parallel current," $\lambda \equiv \mu_0 \mathbf{J} \cdot \mathbf{B} / B^2$, is initially peaked at 12.5 in the pinch ("concentrated configuration"). In the final state, the toroidal average λ profile has a plateau with $4 \leq \lambda \leq 6$.



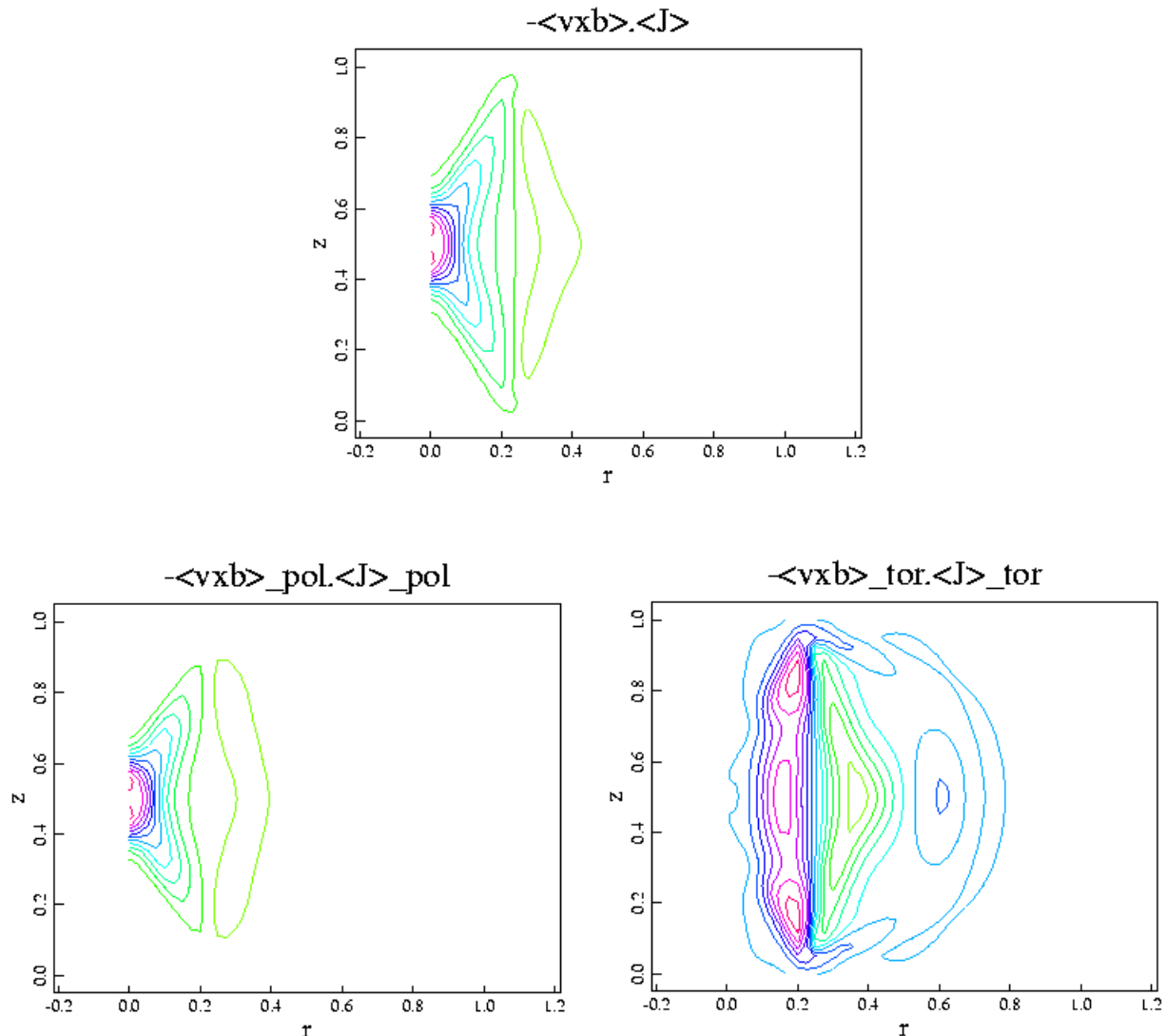
Examining contour plots of local λ shows large variations within the plateau region.



In MHD, fluctuations transfer power from and to the mean field through the correlation of perturbed velocity and magnetic field.

The quantity, $-\langle \mathbf{v}_n \times \mathbf{b}_n \rangle \cdot \langle \mathbf{J} \rangle$, represents energy density transferred between the average current density and Fourier component n . [Ho and Craddock, Phys. Fluids B **3**, 721 (1991).]

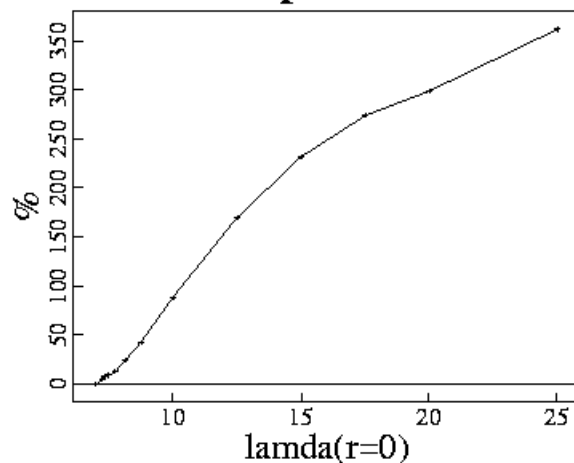
The $n=1$ contribution from the end of the "concentrated configuration" shows power absorbed from average current for $r < 0.22$ and power delivered to average current for $r > 0.22$.



The amount of generated poloidal flux increases with pinch λ , or equivalently applied potential, for a large range of λ in the electrode configuration.

The following plot shows computed flux amplification from a series of simulations with varied $\lambda(r=0)$ of the equilibrium pinch.

Poloidal Flux Amplification vs. Lambda

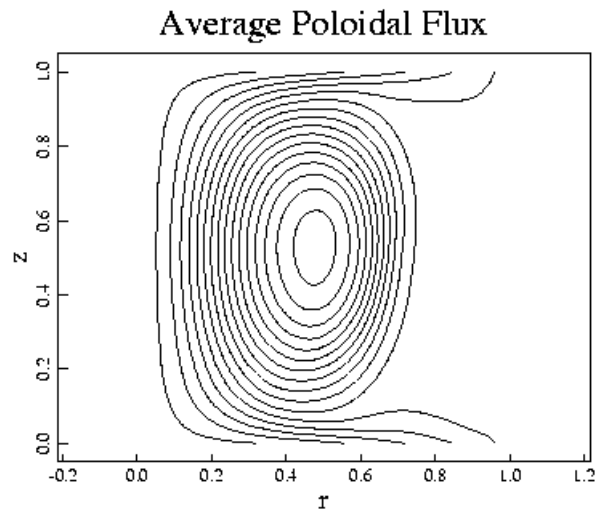


Flux amplification falls to zero at the marginal stability point of the pinch.

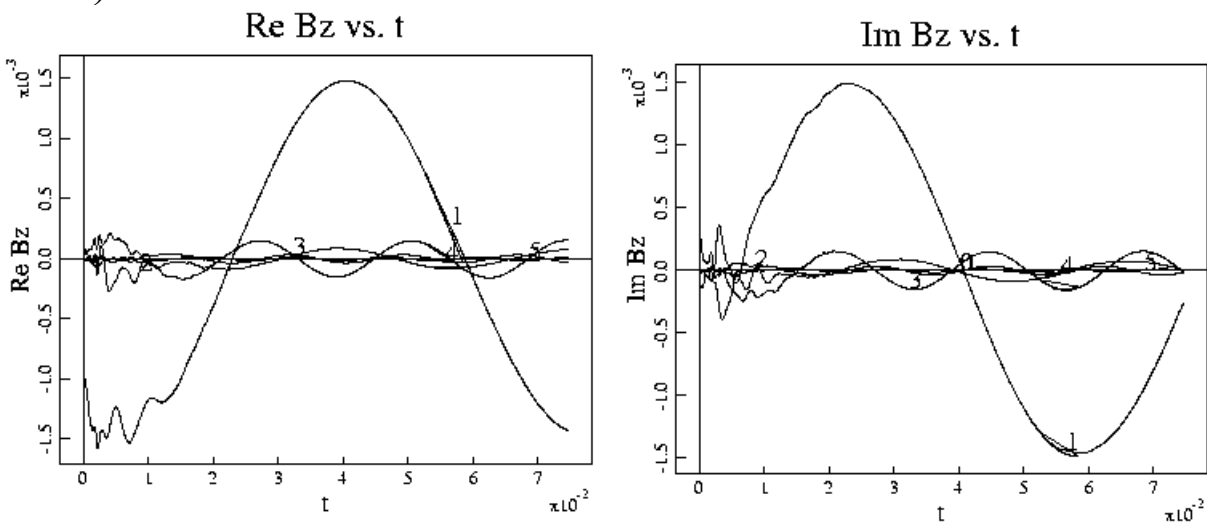
HALL AND ELECTRON INERTIA

The "distributed" configuration has been simulated with Hall and electron inertia terms in Ohm's law.

- With the Hall parameter $(\Omega_{ci}\tau_A)^{-1}$ of $O(10^{-5})$, the result is virtually indistinguishable from the MHD result.
- Increasing the Hall parameter to 0.1 keeping τ_A and τ_r fixed has two effects: 1) average flux contours become skewed,



and 2) the fluctuations rotate in the toroidal direction.

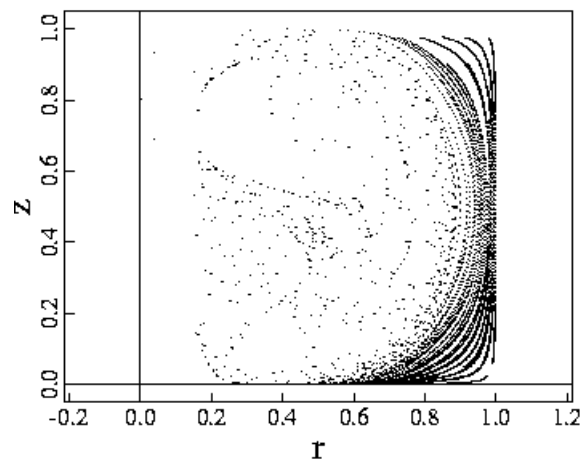


Flux amplification is still within 0.5% of the MHD result.

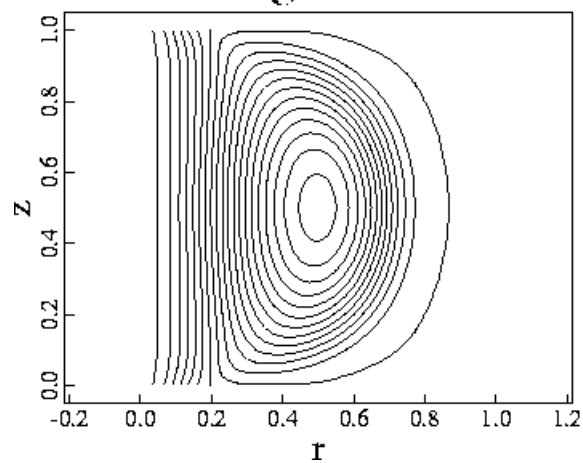
CHOATIC SCATTERING AND FLUX SURFACES

The robust generation of poloidal flux is usually accompanied by chaotic scattering of the magnetic field.

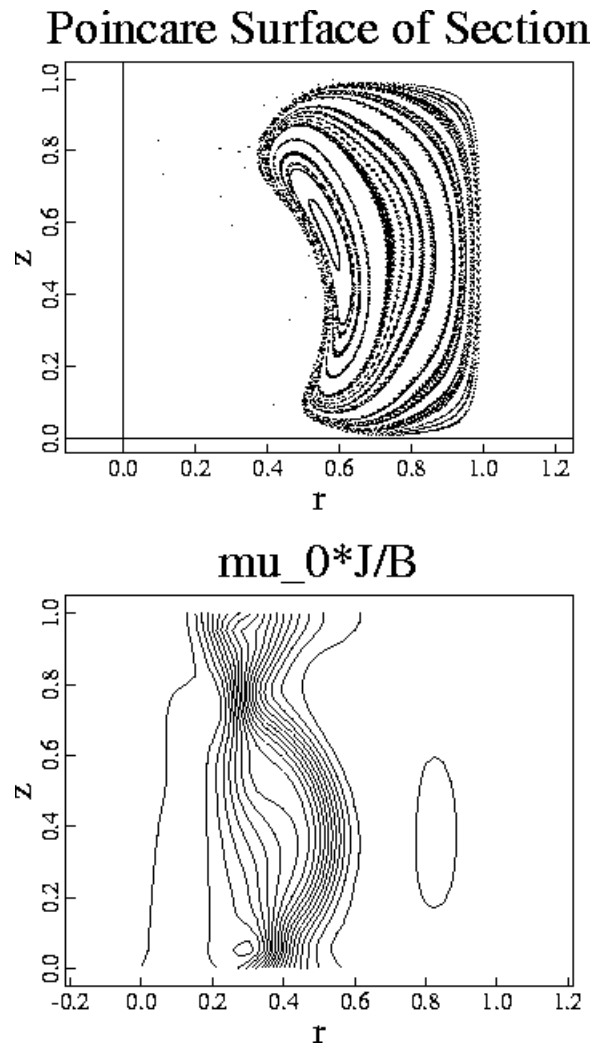
Poincare Surface of Section



Final Average Poloidal Flux

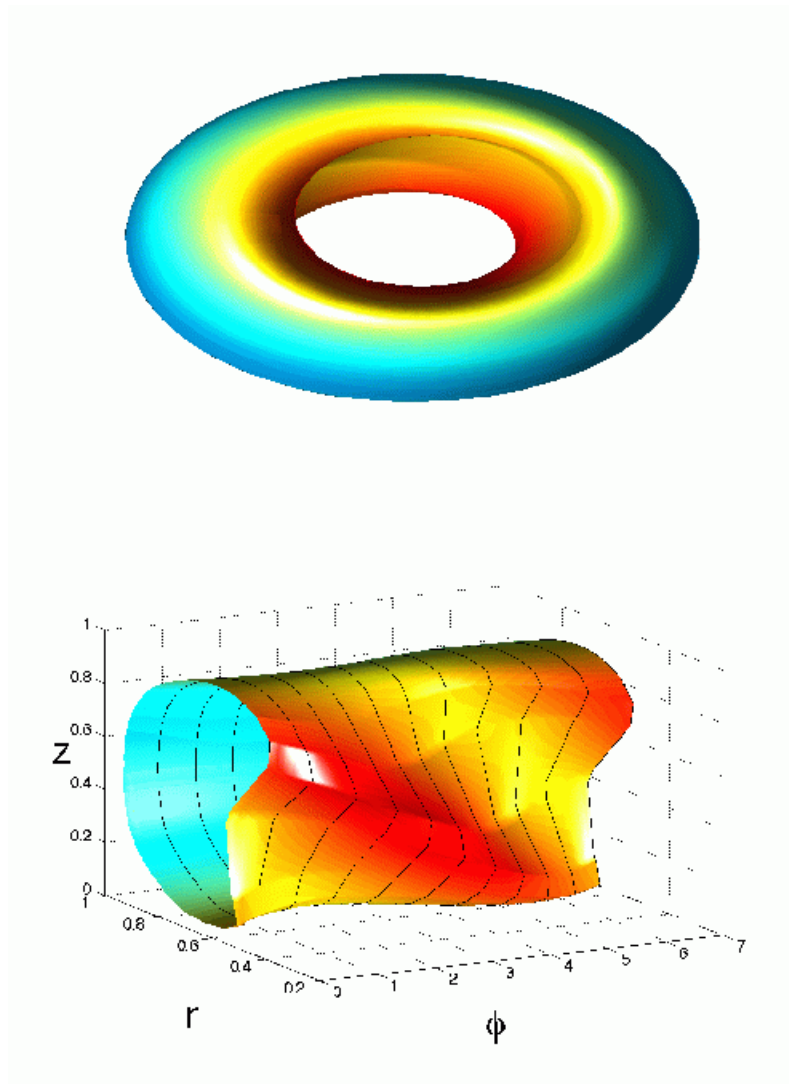


In weakly-driven cases that are just above marginal stability, flux surfaces form and are sustained in steady state.



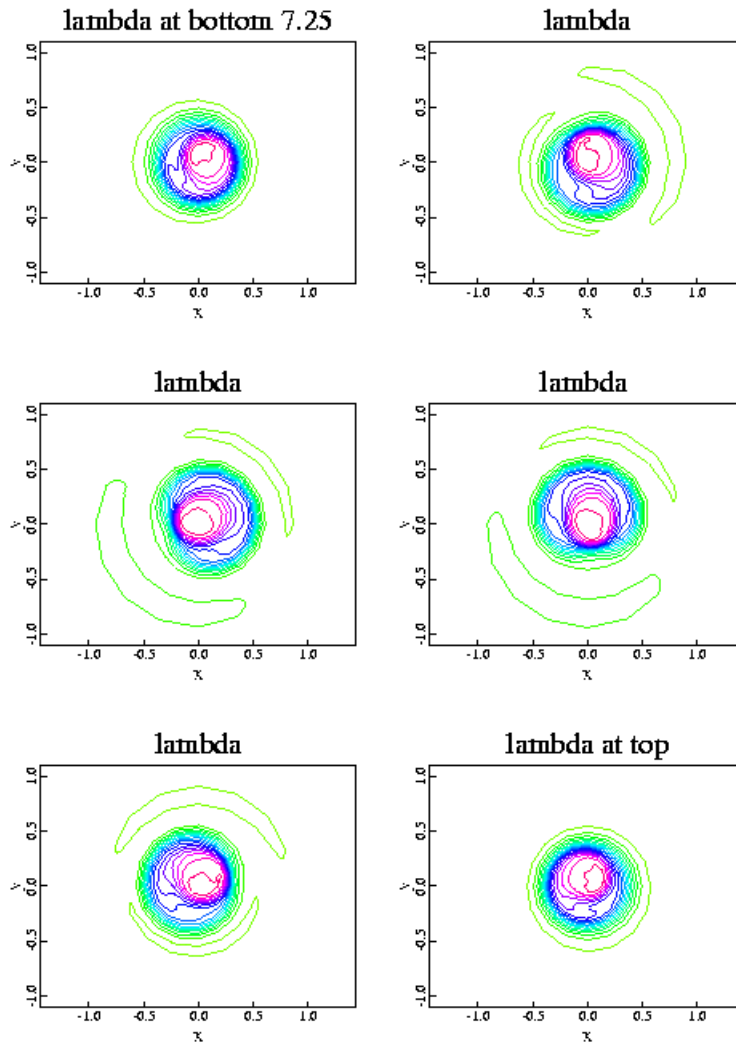
Here the pinch column remains intact and is only helically distorted by the nonlinear saturation.

The helical flux surfaces that form around the distorted current column are analogous to flux surfaces in stellarators. The distorted plasma current column threading the surfaces plays the role of helical external coils in a stellarator.

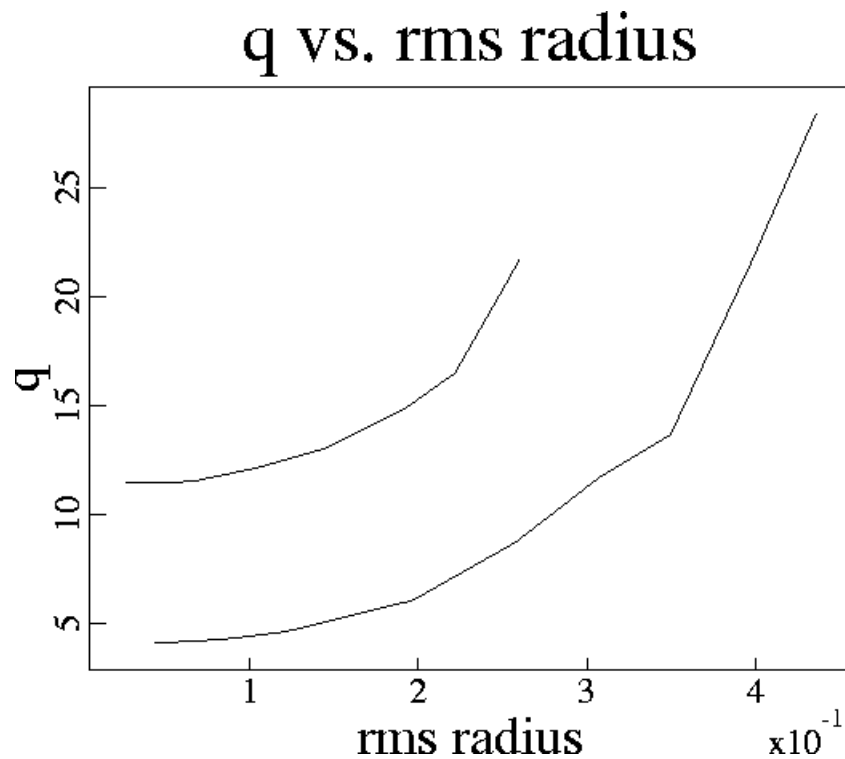


Two views of the same surface are plotted with color indicating radial position to emphasize the helical distortion of the inboard side.

Plots of parallel current at different axial positions show the helical nature of the central current column.



The safety factor of the flux surfaces in a similar case is ~ 10 near the magnetic axis of the structure. q computed with just the symmetric ($n=0$) part of the field is in error by more than a factor of 2.



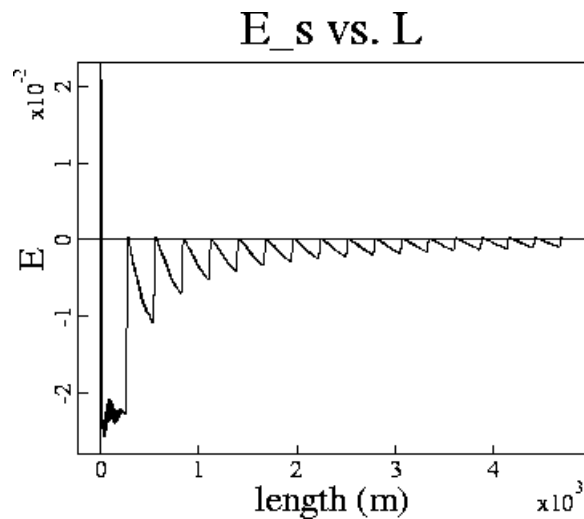
The independent variable is $\langle r^2 \rangle^{1/2}$, mean square distance from the magnetic axis.

In steady state, flux surface averages of the electrostatic field vanish. This is satisfied in the computations.

$$\mathbf{B} \cdot \mathbf{E} = -\mathbf{B} \cdot \nabla \phi = \eta \mathbf{J} \cdot \mathbf{B}$$

$$\phi(L) - \phi(0) = -\int_0^L dl \frac{\eta \mathbf{J} \cdot \mathbf{B}}{B}$$

$$\lim_{L \rightarrow \infty} E_s(L) = 0, \quad E_s(L) \equiv \frac{\int_0^L dl \frac{\eta \mathbf{J} \cdot \mathbf{B}}{B}}{\int_0^L dl \frac{1}{B}}$$

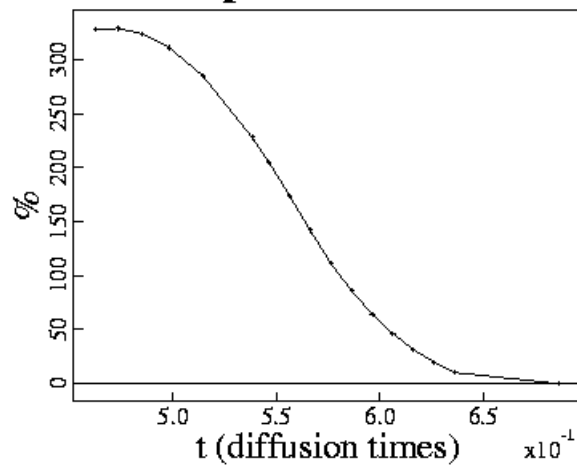


Due to the low current, we would not expect much Ohmic heating within these stellarator-like flux surfaces.

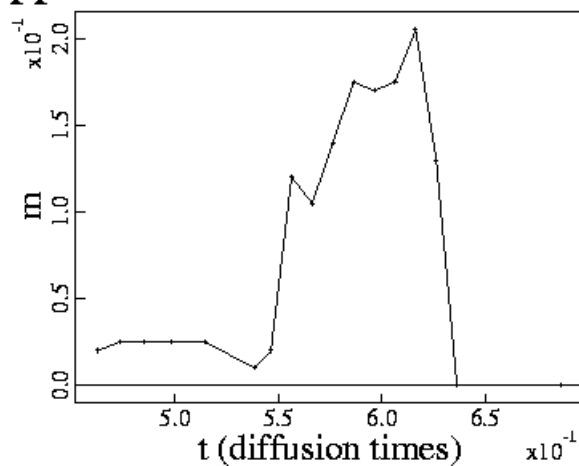
Flux surfaces have also been observed during decay from strongly-driven configurations.

When the applied potential is decreased over $0.1 \tau_r$ in a simulation with $h=1.5$ and uniform flux through the electrodes, flux surfaces form as the poloidal field decays.

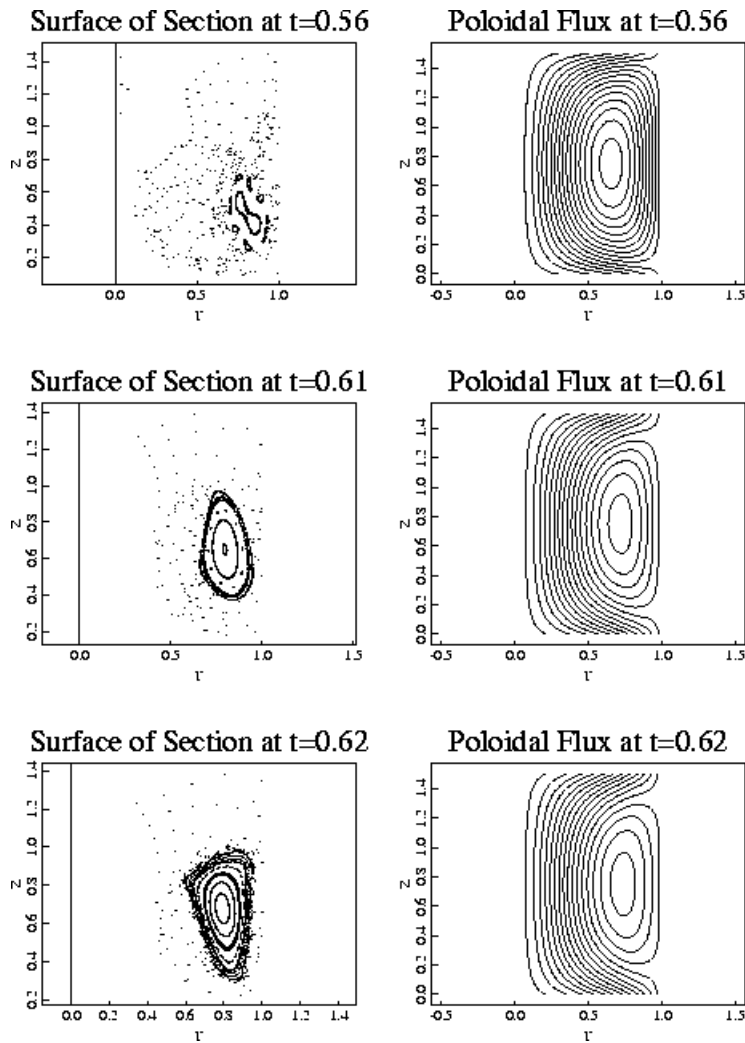
Flux Amplification vs. Time



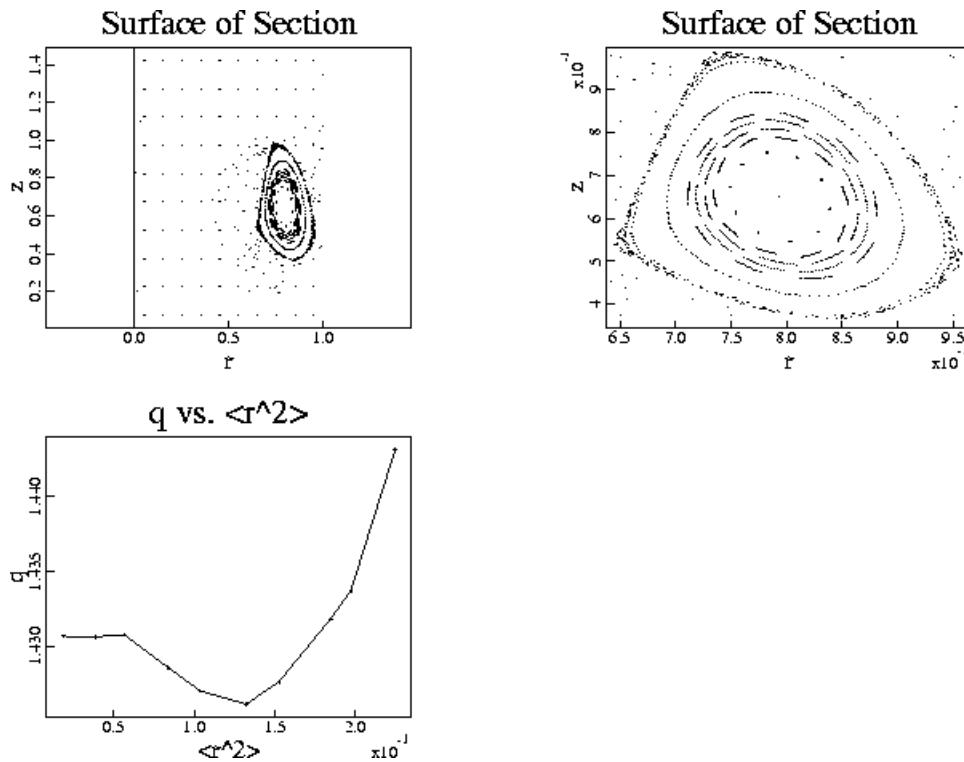
Appr. Island Minor Radius vs. Time



There is net toroidal electric field during the decay, which produces relatively uniform magnetic transform over the flux surfaces. It would also lead to Ohmic heating.



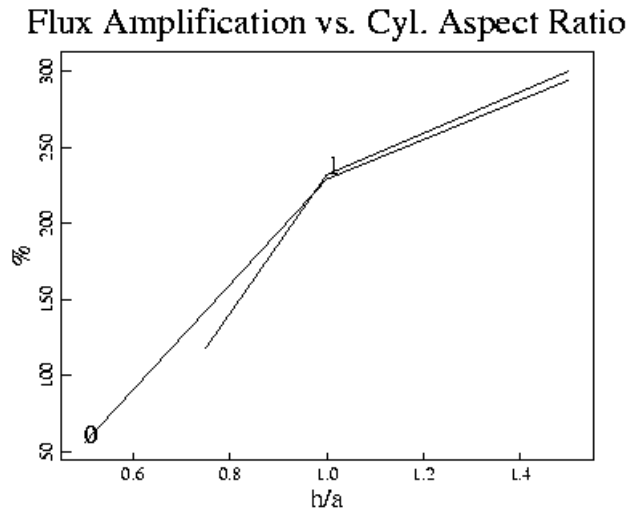
The following shows the safety factor of a structure resulting from decay.



The independent variable in the safety factor plot is $\langle r^2 \rangle^{1/2}$, not $\langle r^2 \rangle$.

VARYING CAN HEIGHT

For a fixed applied electric field, changing the height of the can in the electrode configurations has a large impact on flux amplification.



The curve labeled "0" represents a series of distributed flux simulations, and the curve labeled "1" has concentrated flux. All have an initial pinch $\lambda(r=0)$ of 15.

GUN CONFIGURATION

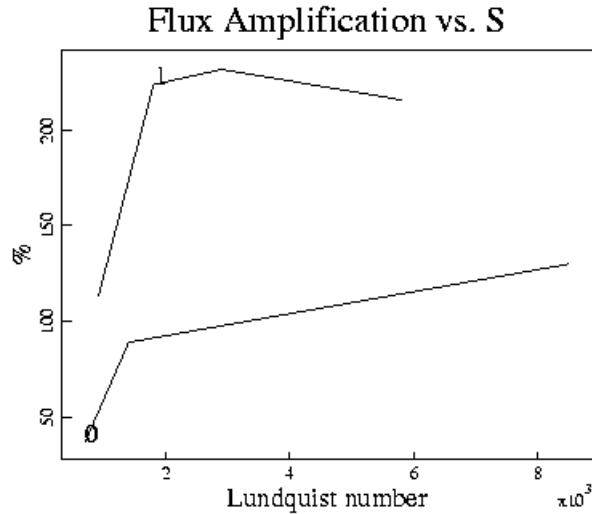
The gun configuration shows at least qualitatively similar behavior to the electrode configurations.

Of the distributed and gun simulations complete to date, input parameters for the two simulations in the following table are most similar.

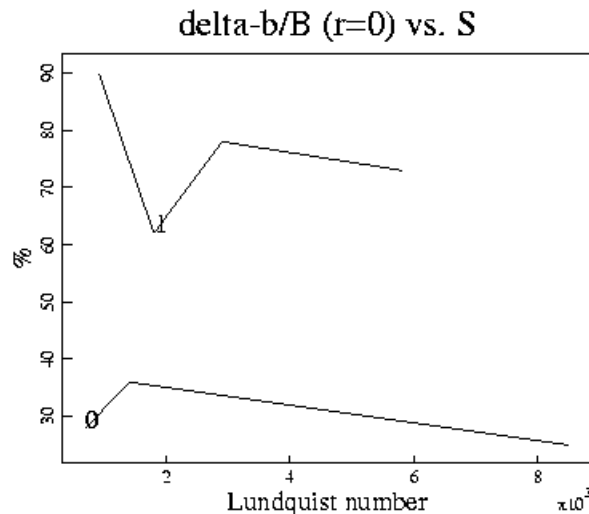
configuration	distributed	gun
applied poloidal flux	0.089	0.10
applied potential	30	42
resulting flux amplification	229%	113%
S based on final peak $ B $ in spheromak	1100	900
peak $\delta b/B$ at $r=0$	36%	90%

LUNDQUIST NUMBER

As S is varied over values of $O(10^3)$ to $O(10^4)$, flux amplification increases.



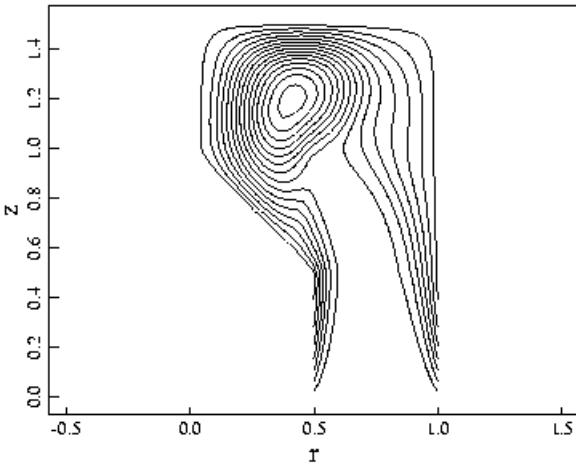
The two curves show the concentrated configuration (label "0") at initial pinch $\lambda=10$ and the gun configuration (label "1") with a value of 42 for the applied potential. In both simulation series, S is varied by changing mass density.



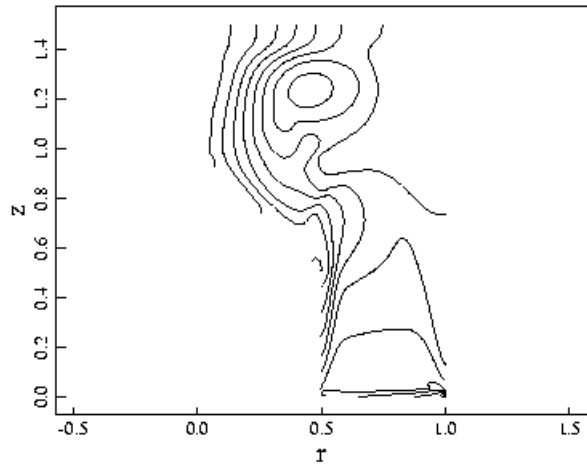
Fluctuation scaling is a critical issue, but the S values used so far are too low to make any predictions about high- S scaling.

As S is increased in the gun configuration, more average poloidal current is entrained with the spheromak.

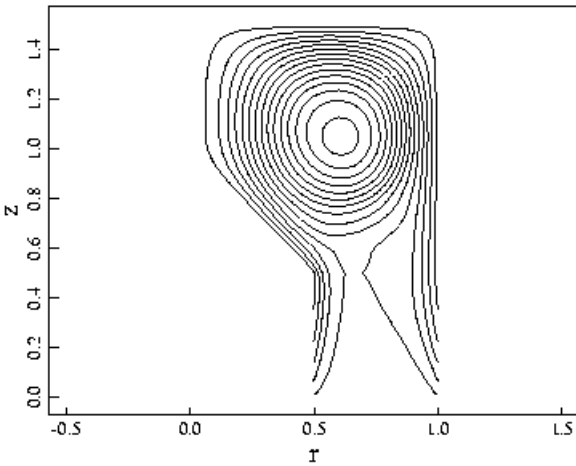
Average Poloidal Flux, $S=900$



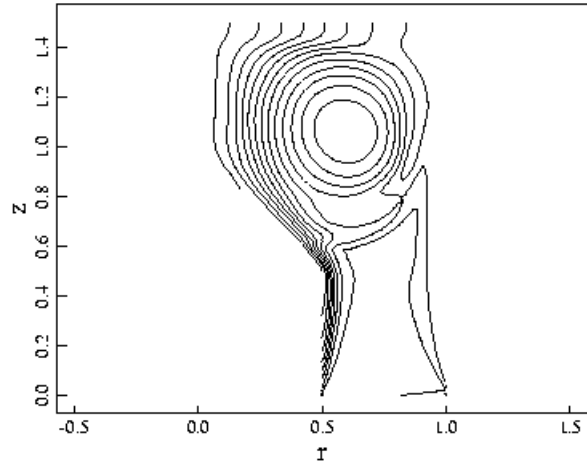
Average $R*B_{\Phi}$, $S=900$



Average Poloidal Flux, $S=2900$



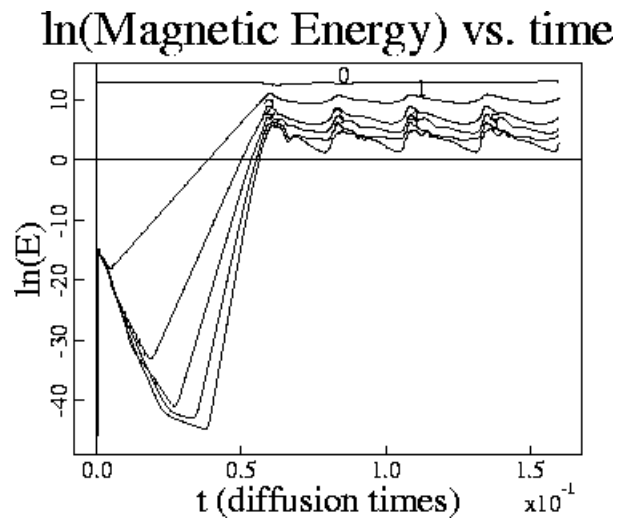
Average $R*B_{\Phi}$, $S=2900$



LIMIT CYCLE BEHAVIOR

In cases with S greater than ~ 3000 , a limit cycle is observed in the temporal evolution as the spheromak is being sustained. This occurs in the electrode and gun configurations.

The evolution of the magnetic energies of the different Fourier components in the $S=8500$ electrode simulation demonstrates this behavior.

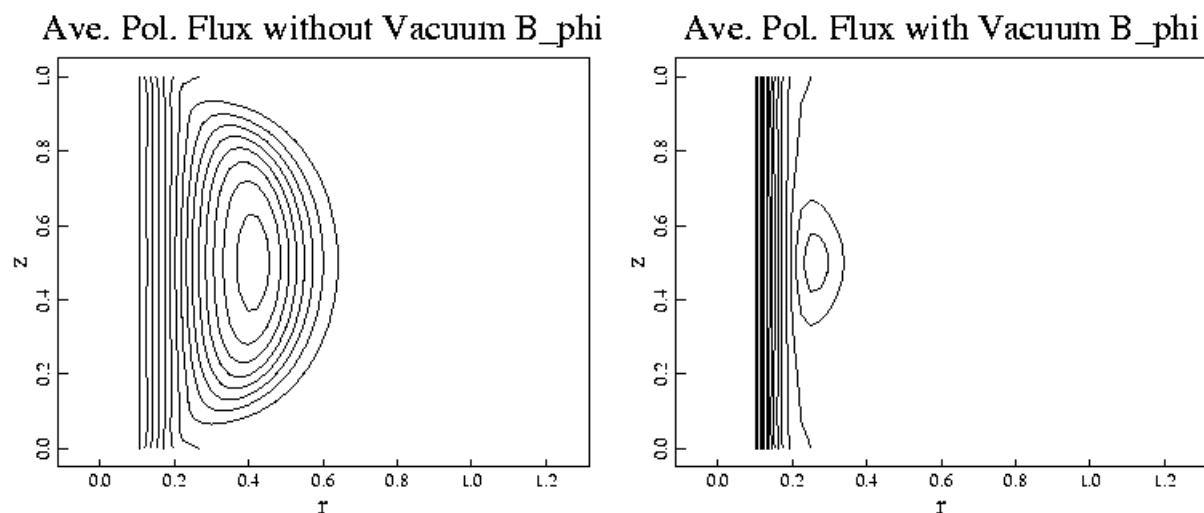


Small islands form at the low perturbed- b point of the cycle.

TRANSITION TO HELICITY INJECTED TOKAMAKS

When the domain is modified to a toroidal configuration, vacuum toroidal field may be added. A study of the transition from spheromak-like configurations to low aspect ratio tokamaks is now underway.

- The first set of these simulations has $R/a=1.1$ and a "concentrated" divertor flux configuration.
- A simulation without toroidal field produces 144% flux amplification with the central column, while a simply connected domain with the same linked poloidal flux and applied potential produces 232% flux amplification.
- With the same poloidal current extracted through the plasma and an additional 43% in the central column, flux amplification drops dramatically to 19%.



- Larger S values and larger applied potentials may be needed.

DISCUSSION AND CONCLUSIONS

- MHD simulations show that spheromaks are generated and sustained as the result of saturation of a current gradient-driven instability in pinch configurations.
- Many different parameters and configurations produce qualitatively the same behavior. This is consistent with the general findings of many experimental programs.
- Initial findings indicate that the Hall term does not influence the sustainment process or fluctuation level, at least up to a Hall parameter of 0.1. However, simulations with gyroviscous effects and larger values of the Hall parameter should be performed.
- Flux surfaces are observed in two different conditions:
 - Low current cases exhibit stellarator-like transform from current in the kinked pinch.
 - Decaying spheromaks show flux surfaces with net current. The plasma within these surfaces would have relatively good confinement, and it would be Ohmically heated. This may have bearing on the 400 eV temperatures observed during the decay phase of the CTX spheromak [Jarboe, et al., Phys. Fluids B **2**, 1342 (1990)].

- Gun and electrode configurations produce qualitatively the same behavior. Topologically, the configurations are the same, so this is an expected result. Lower levels of flux amplification with a gun for similar parameters may result from power loss as current traverses from the gun to the confinement region. The relative performance of the different simulated configurations may not reflect experiment, due to non-MHD effects.
- Investigation of the transition from spheromak-like configurations to helicity injected, low aspect ratio tokamaks is beginning.

This poster will be available on our web site, <http://nimrodteam.org> or <http://nimrod.saic.com> .